AGE-STRUCTURED MODELING OF HEMATOPOIESIS

JOSEPH M. MAHAFFY *

Abstract. Age-structured models for hematopoiesis allow the study of several dynamic hematological diseases and the effects of a phlebotomy in normal human subjects. The method of characteristics with several simplifying assumptions reduces the age-structured model to a system of delay differential equations, which is analyzed for Hopf bifurcations and is more easily simulated. The model can explain the appearance of oscillations in erythrocyte counts in rabbits with an induced auto-immune hemolytic anemia. The model can match cumulative data following a blood donation, but falls short of predicting a normal individual due to other feedback controls.

Key words. Age-structured models, hematopoiesis, periodic diseases, erythropoiesis, delay differential equations, method of characteristics, Hopf bifurcation.

1. Introduction. Age-structured mathematical models provide an effective means of understanding various biological phenomena for large populations. Hematopoiesis is the process by which stem cells residing primarily in the bone marrow, spleen, and liver proliferate and differentiate into the major types of blood cells. Thus, hematopoiesis with its many stages of development lends itself naturally to age-structured modeling and has been studied by numerous researchers in this manner [3, 16, 29, 30, 44, 48, 49, 52].

Various other modeling techniques have been applied to hematopoietic systems, including compartmental models [61, 62, 63, 64, 77], stochastic models [37, 41, 54, 71, 72], and delay differential equations [2, 32, 33, 42, 43, 44, 46, 75]. This survey shows a connection between the age-structured models and delay differential equation models [3, 44, 48, 49]. The age-structured models relate more easily to the biological system, while the delay differential equations are easier to analyze mathematically.

Our interest in studying mathematical models for hematopoiesis centers on two areas. The first area of study examines dynamic hematological diseases [17, 26, 32, 44, 45, 59], where one or more of the circulating hematopoietic cell lines oscillate. Examples of these periodic hematological disorders include cyclical neutropenia [12, 13, 32, 35, 39, 62, 64, 79, 80], chronic myelogenous leukemia [9, 14, 22, 25, 36, 50, 51, 60, 65, 76], periodic auto-immune hemolytic anemia [28, 56, 58], polycythemia vera [53], and cyclical thrombocytopenia [5, 6, 8, 10, 15, 18, 27, 40, 66, 70, 74, 78]. It is likely that abnormalities in the regulatory control processes result in the observed oscillatory phenomena, but often the defective mechanisms are not known.

A second area of study looks at the normal production of red blood cells, erythropoiesis, to determine if a mathematical model might be used to

---

optimize the collection of blood. The disease AIDS has caused great public alarm in the blood supplies. Though tremendous gains have been made in protecting the safety of the blood supplies, there are many times when the national blood supply is low. A mathematical model might suggest ways to improve the rate of collection from the current eight week time table between blood donations or increase the amount of blood collected from autologous donors, who donate for their own elective surgery.

This review article provides a brief summary of the physiological processes for erythropoiesis, then transforms this descriptive biological model into an age-structured model. Next several simplifying assumptions allow the reduction of the age-structured model to a system of delay differential equations, using the method of characteristics. A Hopf bifurcation analysis shows how this model can produce oscillatory behaviors. In Section 4, the system of delay differential equations has its parameters identified by comparison to experimental data in the literature for both a rabbit with an induced auto-immune hemolytic anemia and normal human males following a phlebotomy. Finally, a discussion follows to summarize the results of our modeling efforts to date.

2. The Physiology and an Age-Structured Model. Hematopoiesis begins from a population of undifferentiated stem cells, primarily in the bone marrow, spleen, and liver. Under the influence of many growth factors and hormones, some stem cells divide and become committed to a specific cell type, such as erythrocytes, granulocytes, lymphocytes, monocytes, or platelets. Once a stem cell differentiates into a particular cell type, then several lineage-specific hormones promote rapid cellular proliferation or decrease preprogrammed cell death (apoptosis) to control these cell quantities. The granulocytic pathway leads to different cell types in the immune system. If the stem cell becomes a megakaryocyte, then the cell increases in size undergoing only nuclear division until the cell reaches maturity and separates into thousands of platelets, which are used for the clotting of blood. By volume the largest hematopoietic system produces the erythrocytes, whose primary function is the transport of O_2 to the tissues. The growth and differentiation of these cell lines use complicated hormonal controls, which under abnormal circumstances may result in one of the diseased states listed in the introduction.

For development of the mathematical model, the physiology for erythropoiesis is described in some detail. (See William's Hematology [20] for more details.) Oxygen is vital for generating energy in the tissues of all mammals, and erythrocytes supply most tissues with this O_2, using the protein hemoglobin. There are 3.5×10^{11} erythrocytes for each kilogram of body weight, so almost 7% of the body mass is red blood cells. The turnover rate is about 3×10^9 erythrocytes/kg of body weight each day, which must be carefully regulated by several O_2 sensitive receptors and a collection of growth factors and hormones.
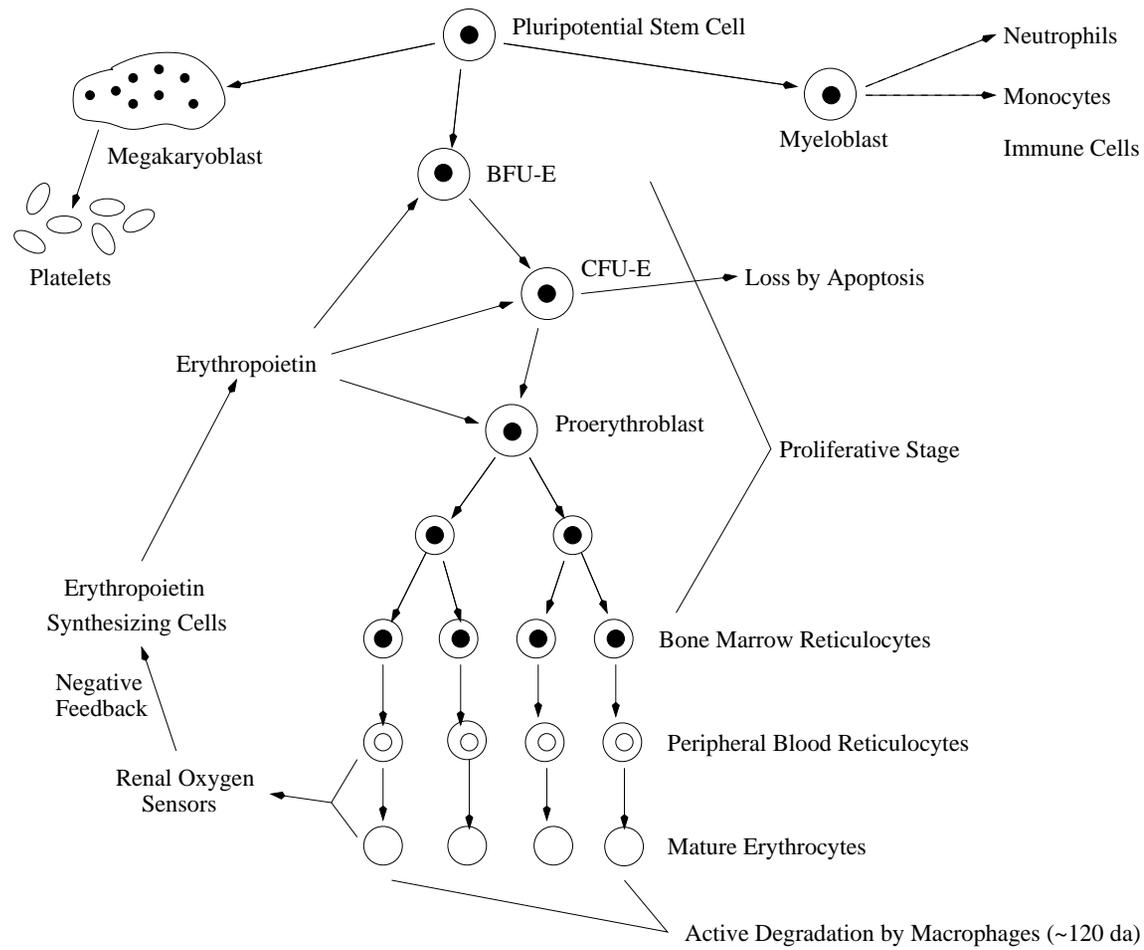
FIG. 2.1. *An overview of erythropoiesis.*

Erythrocytes are not a self-sustaining group of cells, and in fact, they do not even possess a nucleus for DNA replication or transcription. Fig. 1.1 provides an overview of erythropoiesis. This process begins with the pluripotential stem cells, which can produce a variety of cell types. Under the influence of certain hormones, some of the stem cells differentiate into burst forming units, BFU-E, which may form a temporary self-sustaining pool or may proliferate and further differentiate into colony forming units, CFU-E. The CFU-E are a critical stage in the erythroid line that requires adequate supplies of the hormone erythropoietin or EPO. Many BFU-E enter the CFU-E stage of development, but only a fraction receive sufficient EPO to continue their rapid proliferation. The remaining CFU-E apparently self-destruct in the process known as apoptosis. For the next few generations the erythroblasts continue cellular division at approximately 8 hr intervals under the influence of EPO and other hormones, completing 11 or 12 cell cycles. During these divisions, the cell decreases in size and becomes more specialized by increasing hemoglobin concentrations and losing general cellular organelles.

After about 4 days the erythroblast has matured into a reticulocyte. For the next couple of days, the cell ceases mitotic divisions and concentrates on producing hemoglobin, while other cellular components degenerate. This phase of development appears to be largely independent of EPO concentrations. The reticulocytes continue to shrink in size and eventually squeeze out of the bone marrow into the blood stream and circulate throughout the body. Within the first couple of days, the circulating reticulocytes eject their nuclei and form mature erythrocytes, which are functionally a collection of hemoglobin molecules surrounded by a cellular membrane.

Mature erythrocytes are larger in diameter than the capillaries that feed the tissues of the body, so these cells must squeeze through to deliver their O_2 from the lungs. The process of deforming the membrane results in some damage, which cannot be repaired without the nuclear machinery in place. After about 120 days, most of the red blood cells have sufficient damage to their cell membranes that they lose pliability, so are marked by antibodies for destruction by the macrophages (a cell type produced by granulopoiesis). This active degradation results in about 90% of the erythrocytes being destroyed within 15 days either side of 120 days from when they entered the blood stream. Most of the other cells are destroyed earlier by physical movement, which breaks capillaries, impact, such as the crushing force on feet caused by running, or high velocity impact with the walls in major arteries like the aorta.

The circulating erythrocytes carrying O_2 are monitored by special sensory cells located primarily in the peritubular interstitial cells of the outer cortex of the kidneys. Based on the availability of O_2, these specialized renal cells release EPO in the blood via a negative feedback mechanism. Thus, O_2 inhibits the release of EPO, while EPO in the blood bathing

the progenitors of the red blood cells in the bone marrow stimulates differentiation and proliferation. Clearly, this is an over-simplification of the process of erythropoiesis as significant factors such as dietary iron and other hormones have not been discussed, yet are known to play crucial roles.

Our mathematical model is developed from the ideas described above and follows the techniques of Bélair et al. [3] and Mahaffy et al. [48]. Additional material on the development and analysis of age-structured models can be found in Cushing [11], Gurney and Nisbet [31, 55], and Metz and Diekmann [52].

Mahaffy et al. [48] develop an age-structured model for erythropoiesis based on precursor cells, $p(t, \mu)$, with time t and age μ and mature cells, $m(t, \nu)$, with time t and age ν, controlled by the hormone EPO, $E(t)$. If a variable velocity of aging dependent on E, $V(E)$, affects the precursor cell with mature cells simply aging with time t, then the partial differential equations describing p and m are given by:

$$(2.1) \qquad \frac{\partial p}{\partial t} + V(E)\frac{\partial p}{\partial \mu} = V(E)[\beta(\mu, E) - \alpha(\mu, E) - H(\mu)]p,$$

$$t > 0, \quad 0 < \mu < \mu_F,$$

$$(2.2) \qquad \frac{\partial m}{\partial t} + \frac{\partial m}{\partial \nu} = -\gamma(\nu)m,$$

$$t > 0, \quad 0 < \nu < \nu_F(t),$$

where $\beta(\mu, E)$ is the birth rate for proliferating precursor cells, $\alpha(\mu, E)$ represents the death rate from apoptosis, and $H(\mu)$ is the disappearance rate function for precursor cells that mature with

$$H(\mu) = \frac{h(\mu - \bar{\mu})}{\int_\mu^{\mu_F} h(s - \bar{\mu})ds}$$

and

$$\int_0^{\mu_F} h(\mu - \bar{\mu})d\mu = 1.$$

The function $\gamma(\nu)$ represents the death rate of mature cells.

The boundary conditions for the model are given by:

$$(2.3) \qquad V(E)p(t, 0) = S_0(E),$$

$$(2.4) \qquad m(t, 0) = V(E)\int_0^{\mu_F} h(\mu - \bar{\mu})p(t, \mu)d\mu,$$

$$(2.5) \qquad (1 - \dot{\nu}_F(t))m(t, \nu_F(t)) = Q,$$

where $S_0(E)$ represents the recruitment of stem cells into the precursor population, μ_F represents the maximum age for a precursor cell to reach maturity, and Q is a fixed erythrocyte removal rate. This last boundary

condition assumes preferrential removal of the oldest cells at a constant rate by the macrophages and was derived in Mahaffy *et al.* [48].

The renal sensors detect the partial pressure of O_2 in the blood, which we assume is directly proportional to the total population of erythrocytes, provided the blood volume remains relatively constant. The O_2 carrying ability of the blood is found by integrating over all the age classes of $m(t, \nu)$, giving the total population of erythrocytes:

$$(2.6) \qquad M(t) = \int_0^{\nu_F(t)} m(t, \nu) d\nu.$$

The concentration of EPO, $E(t)$, is governed by the differential equation:

$$(2.7) \qquad \frac{dE}{dt} = f(M) - kE,$$

where $f(M)$ represents the rate of production of EPO and the last term in (2.7) represents degradation of EPO. The negative feedback function $f(M)$ is a monotone decreasing function of M and is assumed to have the form

$$(2.8) \qquad f(M) = \frac{a}{1 + KM^r},$$

which is a Hill function that often occurs in enzyme kinetic problems.

3. Mathematical Analysis of the Model. Mahaffy *et al.* [48] reduce the age-structured model given by Eqns. (2.1)–(2.7) to a system of threshold delay equations following the techniques of several authors [3, 23, 24, 52, 67]. The technique assumes that $E(t)$ is known, then the method of characteristics is used to find $p(t, \mu)$ and $m(t, \nu)$. Several simplifying assumptions are necessary to reduce the model to a system of delay differential equations. In this review paper we introduce the simplifying assumptions first, then by using the method of characteristics, a system of delay differential equations with a fixed delay in one equation and a state-dependent delay in another is derived. Below we demonstrate the method of characteristics and show how the age-structured model and delay differential equations are related.

The most important assumption needed in the reduction of the age-structured model to a system of delay differential equations is that the velocity of aging for the precursor cells is constant, so we assume $V(E) = 1$. There is experimental evidence that under stress conditions with high levels of EPO, the precursor cells can mature more rapidly [21, 34, 38, 57], so this is also the weakest assumption. The second assumption is that the precursor cells grow exponentially for a given period of time μ_1, then stop dividing, so

$$(3.1) \qquad \beta(\mu, E) = \left\{ \begin{array}{ll} \beta, & \mu < \mu_1, \\ 0, & \mu \geq \mu_1, \end{array} \right.$$

for some constant growth rate β. We ignore apoptosis, $\alpha(\mu, E)$, and assume that this occurs primarily in the earliest stages of precursor development, so can be easily absorbed into $S_0(E)$ in the boundary condition (2.3). We assume that $h(\mu - \bar{\mu})$ is a delta function, so that all the precursors mature at the same age, μ_F. Finally, we assume the decay rate $\gamma(\nu)$ is constant and denoted by γ.

The simplified model now satisfies the partial differential equations:

(3.2) $$\frac{\partial p}{\partial t} + \frac{\partial p}{\partial \mu} = \beta(\mu, E)p,$$

(3.3) $$\frac{\partial m}{\partial t} + \frac{\partial m}{\partial \nu} = -\gamma m.$$

The boundary conditions are

(3.4) $$\begin{aligned} p(t, 0) &= S_0(E), \\ p(t, \mu_F) &= m(t, 0), \\ (1 - \dot{\nu}_F(t))m(t, \nu_F(t)) &= Q. \end{aligned}$$

The equation for EPO concentration is unchanged, so satisfies:

(3.5) $$\dot{E} = \frac{a}{1 + KM^r} - kE,$$

where $M(t) = \displaystyle\int_0^{\nu_F(t)} m(t, \nu)d\nu$.

3.1. Method of Characteristics. Eqns. (3.2) and (3.3) are linear first order hyperbolic partial differential equations. The method of characteristics is used to transform the partial differential equations of the model into an easily solvable ordinary differential equation. Begin by parameterizing the independent variables t and μ by one variable s. Then $p(t(s), \mu(s)) = P(s)$. From the chain rule, we have

(3.6) $$\frac{dP}{ds} = \frac{\partial p}{\partial t}\frac{dt}{ds} + \frac{\partial p}{\partial \mu}\frac{d\mu}{ds} = \beta(\mu(s))P(s),$$

which is a linear ordinary differential equation. If

(3.7) $$\frac{dt}{ds} = 1 \qquad \text{and} \qquad \frac{d\mu}{ds} = 1,$$

then (3.6) has the solution

(3.8) $$P(s) = p(t, \mu) = P(0)\exp\left[\int_0^s \beta(\mu(r))dr\right].$$

The solution of (3.7) creates the characteristic lines along which (3.8) is valid. Fig. 3.1 illustrates these simple characteristics. For $t < \mu$, $t(s) = s$

and $\mu(s) = \mu_0 + s$. For $t > \mu$, $t(s) = t_0 + s$ and $\mu(s) = s$. The general solution, (3.8), becomes

$$p(t,\mu) = \begin{cases} p(0,\mu - t)exp\left[\int_0^t \beta(s)ds\right], & t < \mu, \\ p(t - \mu, 0)exp\left[\int_0^\mu \beta(s)ds\right], & t > \mu. \end{cases}$$

By examining only long time behavior with $t > \mu$ and evaluating μ at μ_F, our assumption on $\beta(\mu, E)$ gives

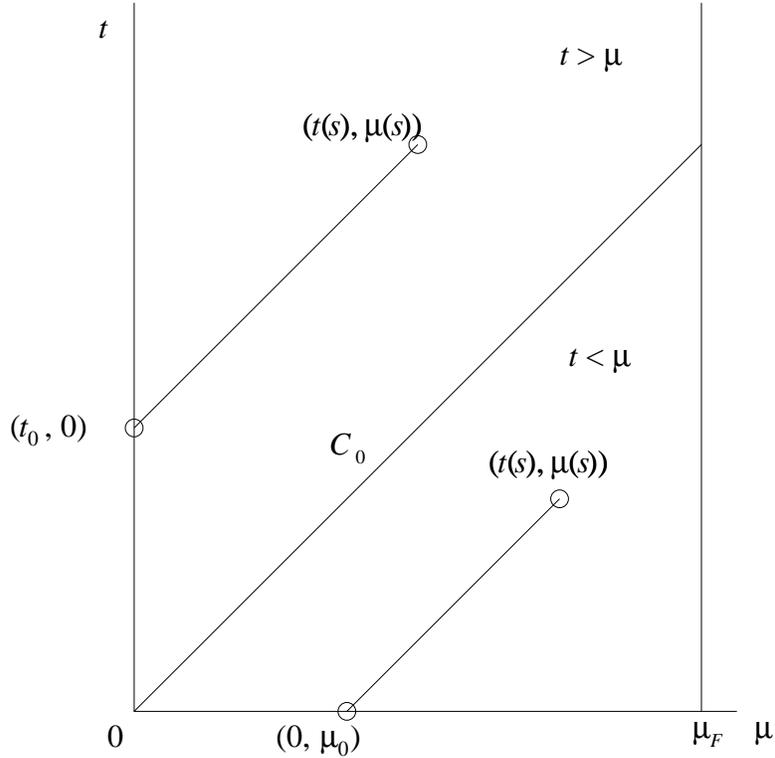$$p(t,\mu_F) = p(t - \mu_F, 0)e^{\beta\mu_1} = e^{\beta\mu_1}S_0(E(t - \mu_F)).$$

FIG. 3.1. *Diagram showing the characteristics for the simplified age-structured model.*

From the form of (3.3), it is easy to see that a very similar set of solutions for $m(t,\nu)$ are obtained using the method of characteristics. Thus,

$$m(t,\nu) = m(t - \nu, 0)e^{-\gamma\nu}, \quad \text{for} \quad t > \nu.$$

From the expression for $M(t)$ and the second boundary condition in (3.4), we obtain

$$M(t) = \int_0^{\nu_F(t)} m(t - \nu, 0)e^{-\gamma\nu}d\nu,$$

$$= \int_0^{\nu_F(t)} p(t - \mu_F - \nu, 0)e^{-\gamma\nu}d\nu,$$

$$= \int_0^{\nu_F(t)} e^{\beta\mu_1} S_0(E(t - \mu_F - \nu))e^{-\gamma\nu}d\nu,$$

$$= e^{-\gamma(t-\mu_F)}e^{\beta\mu_1} \int_{t-\mu_F-\nu_F(t)}^{t-\mu_F} S_0(E(w))e^{\gamma w}dw,$$

where the last integral is obtained by letting $w = t - \mu_F - \nu$ in the previous expression. To obtain a differential equation for $M(t)$, Leibnitz's rule for differentiating an integral gives:

$$\dot{M}(t) = -\gamma e^{-\gamma(t-\mu_F)}e^{\beta\mu_1} \int_{t-\mu_F-\nu_F(t)}^{t-\mu_F} S_0(E(w))e^{\gamma w}dw$$

$$+ e^{-\gamma(t-\mu_F)}e^{\beta\mu_1} \left[S_0(E(t-\mu_F))e^{\gamma(t-\mu_F)} \right.$$

$$\left. - S_0(E(t-\mu_F-\nu_F(t)))e^{\gamma(t-\mu_F-\nu_F(t))}(1 - \dot{\nu}_F(t)) \right]$$

$$= -\gamma M(t) + e^{\beta\mu_1} S_0(E(t-\mu_F)) - Q,$$

from $m(t, \nu_F(t)) = e^{\beta\mu_1} S_0(E(t - \mu_F - \nu_F(t)))e^{-\gamma\nu_F(t)}$ and the constant flux boundary condition (3.4). It is easy to interpret this last expression for $\dot{M}(t)$ from a conservation of mass idea. The second term is the production of new mature cells, which result from the exponential growth of the stem cells that were recruited μ_F units of time earlier. The loss of mature cells come from two sources. The first term represents the random destruction of mature cells throughout their lifetime, while the last term represents the constant flux due to active degradation of the oldest mature cells.

3.2. Delay Differential Equations and Linear Analysis. With the simplifying assumptions above, the method of characteristics eliminates the need of the age-structured populations, p and m, and replaces them with a differential delay equation for the total mature population, $M(t)$. Thus, the system of partial differential equations are replaced with an equivalent system of delay differential equations with the state variables, $M(t)$, $E(t)$, and $\nu_F(t)$. The last variable results from the need to keep track of the length of time that mature cells may live. The differential equation describing its behavior is easily derived from the expression for $m(t, \nu_F(t))$ and the constant flux boundary condition in (3.4). Let $T = \mu_F$, then the following system of delay differential equations with a fixed delay T and a state dependent delay occurring in the equation for ν_F is obtained:

$$\frac{dM(t)}{dt} = e^{\beta\mu_1} S_0(E(t - T)) - \gamma M(t) - Q,$$

$$(3.9) \qquad \frac{dE(t)}{dt} = f(M(t)) - kE(t),$$

$$\frac{d\nu_F(t)}{dt} = 1 - \frac{Qe^{\gamma \nu_F(t)}}{e^{\beta \mu_1} S_0(E(t - T - \nu_F(t)))}.$$

Though initially it appears as if we have replaced a complicated system of partial differential equations with a difficult state-dependent delay differential equation, it is easily seen that the $\dot{\nu}_F(t)$ equation is uncoupled from the other two equations and that the equation for $\dot{M}(t)$ has only the single time delay T. This makes the stability analysis of this system relatively easy.

The stability analysis of (3.9) uses standard techniques. A unique equilibrium, $(\overline{M}, \overline{E}, \overline{\nu}_F)$, exists since $S_0(E)$ is monotonically increasing and $f(M)$ is a negative feedback function. The simplified model given by (3.9) is linearized about its equilibrium, and the resulting linear system is given by:

$$\dot{M}_L(t) = e^{\beta \mu_1} S_0'(\overline{E}) E_L(t - T) - \gamma M_L(t),$$

$$(3.10) \qquad \dot{E}_L(t) = f'(\overline{M}) M_L(t) - k E_L(t),$$

$$\dot{\nu}_{LF}(t) = \frac{1}{\overline{E}} E_L(t - T - \overline{\nu}_F) - \gamma \nu_{LF}(t),$$

where $M_L(t) = M(t) - \overline{M}$, $E_L(t) = E(t) - \overline{E}$, and $\nu_{LF}(t) = \nu_F(t) - \overline{\nu}_F$ are perturbations from the equilibrium. Stability of this system is found using standard techniques from delay differential equations, which means seeking solutions $\mathbf{x}(t) = \boldsymbol{\xi} e^{\lambda t}$ with $\mathbf{x} = [M_L, E_L, \nu_{LF}]^T$, like in ordinary differential equations. The resulting characteristic equation for the eigenvalues corresponding to (3.10) is given by

$$(3.11) \qquad (\lambda + \gamma) \left[(\lambda + \gamma)(\lambda + k) + A e^{-\lambda T} \right] = 0,$$

where $A \equiv -e^{\beta \mu_1} S_0'(\overline{E}) f'(\overline{M}) > 0$. Clearly, one root is $\lambda = -\gamma$, which is the root of (3.11) associated with the behavior from $\nu_F(t)$ and is part of the stable manifold.

3.3. Hopf Bifurcation. Our interest in the loss of stability of the delay differential equation model centers on experiments by Orr *et al.* [56], where they observed oscillations in red blood cell counts for a group of rabbits that were given iso-antibodies to their erythrocytes. From a modeling perspective, this experiment is effectively increasing the random destruction rate γ. The local stability of the delay differential equation model (3.9) about its equilibrium depends on the eigenvalues satisfying (3.11). Since $\lambda = 0$ is not a root of (3.11) for any of the parameters in the biological range, the way that the equilibrium for the model (3.9) can lose stability as its parameters vary is via a Hopf bifurcation.

For a Hopf bifurcation, there must exist parameter values where (3.11) has purely imaginary roots, $\lambda = i\omega$. Thus, the second factor on the left hand side must be zero or equivalently:

$$(3.12) \qquad (\lambda + \gamma)(\lambda + k) = -Ae^{-\lambda T},$$

for $\lambda = i\omega$. A geometrical argument from complex variables examines (3.12) by aligning the magnitudes and arguments of the left and right hand sides as shown in Fig. 3.2. Parametrized by ω, the left hand side of (3.12) traces a parabola with its magnitude monotonically increasing. The right hand side produces a circles of radius A. A Hopf bifurcation occurs where the curves intersect.
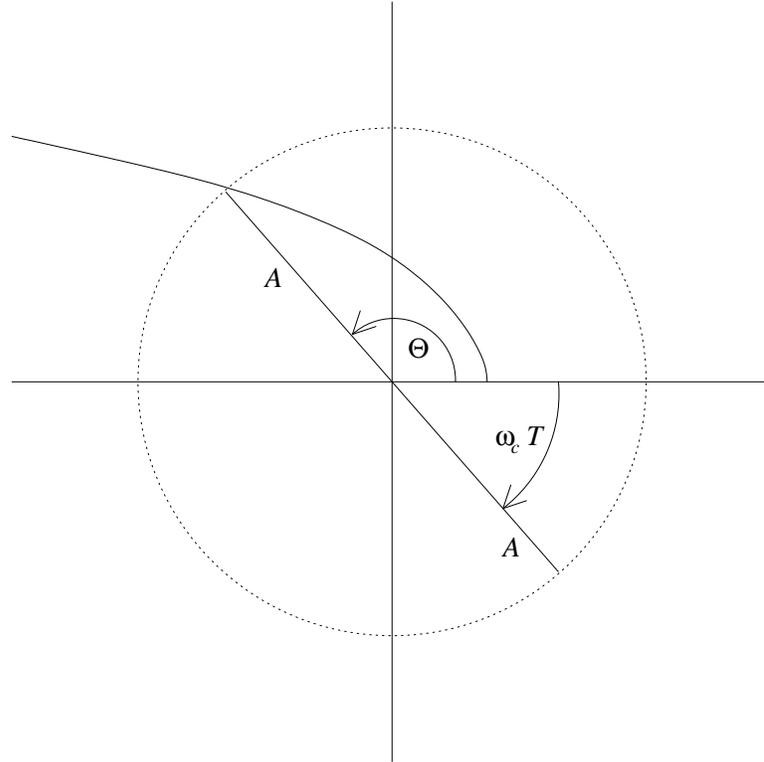

FIG. 3.2. *Geometrical argument for finding a Hopf bifurcation.*

Suppose the destruction rate γ is fixed and that A is allowed to vary. Algebraically, the Hopf bifurcation is found by finding ω_c where the complex arguments agree, so

$$(3.13) \quad \Theta(\omega_c) = \arctan\left(\frac{\omega_c(\gamma + k)}{\gamma k - \omega_c^2}\right) = \pi - \omega_c T, \qquad 0 < \omega_c < \pi/T.$$

Then adjusting A such that the magnitudes agree at the value of ω found in (3.13), so

$$A = \sqrt{(\gamma k - \omega_c^2)^2 + \omega_c^2(\gamma + k)^2}.$$

Bélair [1] showed that for (3.9), this is a supercritical Hopf bifurcation, giving rise to stable periodic solutions.

4. Comparison with Experimental Data. This section examines how well our mathematical model simulates actual experimental data. We chose to consider two experimental situations to test the properties of the mathematical model. The first case is an experiment on rabbits by Orr *et al.* [56] with an induced auto-immune hemolytic anemia. Our second modeling effort is directed at the behavior of the erythropoietic system following a blood donation in a normal human male.

4.1. Auto-Immune Hemolytic Anemia. Orr *et al.* [56] injected a collection of rabbits with an iso-antibody for their erythrocytes every 2–3 days, which produced an induced auto-immune hemolytic anemia. The populations of erythrocytes in these anemic rabbits oscillated about a sub-normal mean population of erythrocytes. Their article ([56], Fig. 3) showed one rabbit with regular oscillations of its erythrocytes around 75% of normal with an amplitude of about 10–15% and a period around 17 days. From a modeling perspective, these experiments are equivalent to increasing the random destruction rate γ in the mathematical model given by (3.9).

In order to simulate the mathematical model and determine where the system undergoes a Hopf bifurcation and loses stability, several of the parameters must be determined. From the observations of Orr *et al.* [56], we chose $\overline{M} = 2.63(\times 10^{11}$ erythrocytes/kg of body weight), which is 75% of normal. Bélair *et al.* [3] used a least squares fit to the data of Erslev [19] to obtain $\overline{E} = 71.1$ (mU/ml). Burwell *et al.* [7] give the lifespan of erythrocytes of rabbits to be 45–50 days, so we took $\overline{\nu}_F = 50$ days. Orr *et al.* [56] estimated the half-life of circulating EPO to be 2.5 hr, based on rats, so we took $k = 6.65$ day^{-1} for rabbits. The nonlinear fit of Bélair *et al.* [3] found the parameters in (3.5) to be $a = 15,600$ (mU/ml/day), $K = 0.0382$, and $r = 6.96$. We assumed $\beta = 2.773$ day^{-1} (cell doubling every 6 hr) and $\mu_1 = 3$ days.

Mahaffy *et al.* [48] used these parameters in (3.9) and adjusted T and γ to yield simulated $M(t)$ close to the one of the experimental rabbits of Orr *et al.* [56]. A reasonable fit was found with $T = 4.1$ days and $\gamma = 0.065$ days^{-1}. These parameters and an equilibrium analysis yield $S_0'(\overline{E}) = 0.0025$ and $Q = 0.0069$. The simulation of (3.9) has a period of 15.9 days with erythrocyte oscillations between 0.67 and 0.91 (fraction of normal) and EPO concentration fluxuating between 20.2 and 154.5 mU/ml. Fig. 4.1 graphically shows our simulation (solid line) with the data (dash-dot line), which is comparable if one ignores the first 40–50 days in what

might be transient effects. The graph suggests that our model can estimate the rate of destruction, γ, for erythrocytes in this experiment. Indirectly, it provides an estimate of the maturation time, T.
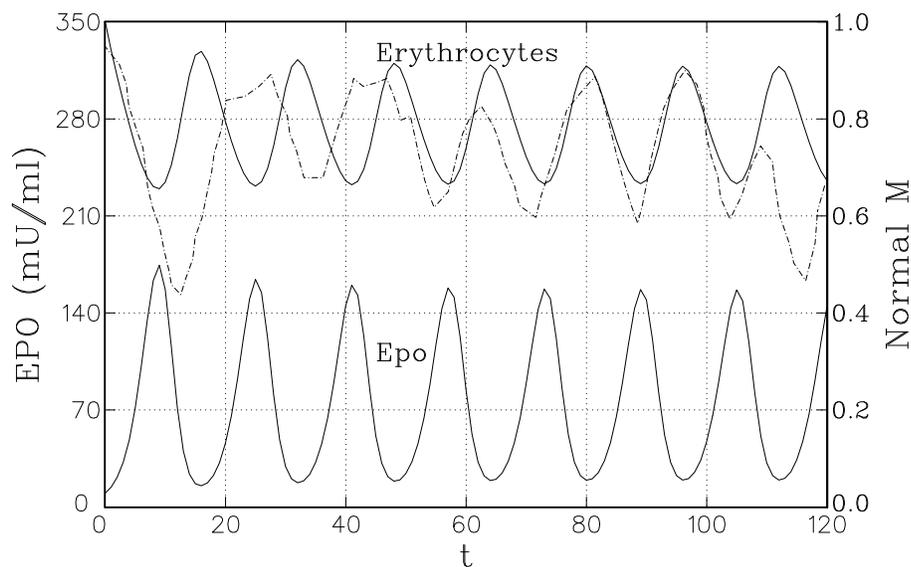

FIG. 4.1. *The age-structured model is given by the solid curve, while the data from Orr et al. is shown with the dash-dot curve.*

4.2. Blood Donation of a Normal Subject. A standard blood donation in the U. S. is 450 g, which represents about 8% of the total blood volume for the average man. About 43% of this blood by volume is erythrocytes with the remainder being mostly plasma. The age-structured model is based on the number of erythrocytes; however, the O_2 sensors in the kidneys probably determine the partial pressure of O_2 in the blood based on the concentration of hemoglobin. (Undoubtedly, its even more complex than this.) The concentration of hemoglobin depends on both the volume of erythrocytes and the volume of plasma.

Blood banks often use optical sensors to find the concentration of hemoglobin and determine whether the subject is eligible to donate blood. Let $Hb(t)$ be the concentration of hemoglobin (g/100 ml of blood). If $M(t)$

is the volume of erythrocytes and $q(t)$ is the plasma volume, then

(4.1) $$Hb(t) \simeq \frac{100}{3} \frac{M(t)}{M(t) + q(t)}.$$

The factor $\frac{100}{3}$ relates a 45% hematocrit (normal), given by $M(t)/(M(t) + q(t)) = 0.45$, to a hemoglobin reading of 15.0 g/100 ml. Note that if erythrocytes are assumed to have a unit volume, then this $M(t)$ is equivalent to the $M(t)$ given in (3.5).

Following a blood donation, blood plasma is regenerated more rapidly than the erythrocytes. (In fact, there is a constant exchange between plasma volume in the tissues and plasma in the blood stream.) Mahaffy *et al.* [49] examined the data of Wadsworth [73] and chose a plasma function

(4.2) $$q(t) = \alpha_1 \left(1 + (\alpha_2 t - 0.08)e^{-\alpha_3 t}\right),$$

where 0.08 reflects the plasma lost at $t = 0$ (time of the phlebotomy). The parameter α_1 is calculated from the equilibrium values $\overline{M}$ and $\overline{Hb}$ in (4.1). The parameters α_2 and α_3 are found using a least squares best fit to the data of Maeda *et al.* [47] and Wadsworth [73].

To study the effects of a phlebotomy, including the loss of blood plasma, Mahaffy *et al.* [49] modified the erythropoietic model given by (3.9). The new system of delay differential equations becomes:

(4.3)
$$\frac{dM(t)}{dt} = e^{\beta\mu_1} S_0(E(t - T)) - \gamma M(t) - Q,$$
$$\frac{dE(t)}{dt} = f(Hb(t)) - kE(t),$$
$$\frac{d\nu_F(t)}{dt} = 1 - \frac{Qe^{-\beta\mu_R}e^{\gamma\nu_F(t)}}{S_0(E(t - T - \nu_F(t)))},$$

where f has the same form as (2.8) and $Hb(t)$ is found from Eqns. (4.1) and (4.2). This system of delay differential equations is readily simulated using an adaptation of the fourth order Runge-Kutta for ordinary differential equations, which simplifies our problem of fitting parameters in the model to the experimental data.

Wadsworth [73] and Maeda *et al.* [47] collected data on hemoglobin concentrations for normal human males following a phlebotomy for an extended period of time. Maeda *et al.* [47] also collected data on the EPO concentrations of their subjects. Many of the parameters are determined from the literature, and the remainder were found by using a least squares best fit to the data of Wadsworth [73] and Maeda *et al.* [47]. Details on finding the parameters can be found in Mahaffy *et al.* [49]. For our simulation, we assumed that $\overline{Hb} = 15.29$ (g/100 ml), $\overline{E} = 16.95$ (mU/ml), and $\overline{\nu}_F = 120$ (days). Since $\overline{M} = 3.5$, $\alpha_1 = 4.13$. From the information in the literature, we chose $\beta = 2.079$ (days^{-1}), $\mu_1 = 4.0$ (days), $T = 6$ (days)

and $\gamma = 0.001$ (days^{-1}). With the assumption that $S_0(E)$ is linear, a steady-state analysis of (4.3) yields $S_0(E) = 4.45 \times 10^{-7}E$ and $Q = 0.0275$. With $r = 7$, the least squares best fit yields $\alpha_2 = 0.05421$, $\alpha_3 = 0.1214$, $a = 198.1$, and $K = 9.262 \times 10^{-9}$. We constrained the half-life of EPO to be between 4 and 24 hr, and the least squares functional was minimized at $k = 4.16$ (days^{-1}), corresponding to the shortest EPO half-life allowed.
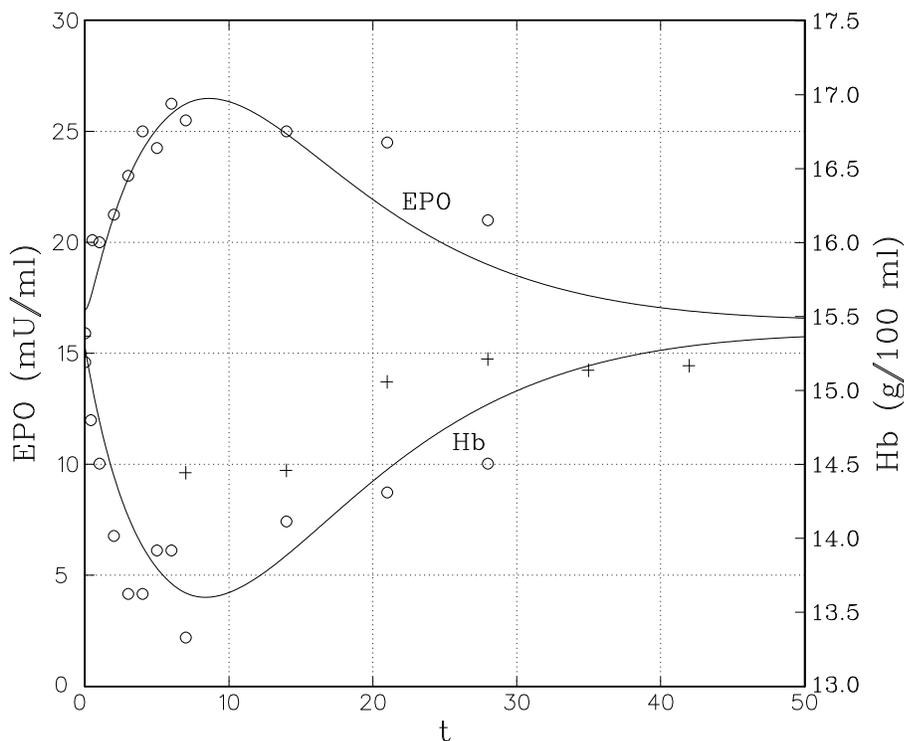

Fig. 4.2. *The graph shows the behavior of the mathematical model for a normal male subject following a phlebotomy, while the data are shown for comparison.*

With the parameters given above, the mathematical model (4.3) is simulated for 60 days. The results are shown in Fig. 4.2 with the experimental data. The simulation fits the experimental data reasonably well with a minimum occurring in a little over a week and 90% recovery in about 30 days. Wadsworth [73] (often quoted by blood banks) states "that recovery of haemoglobin concentration was completed within 3–4 weeks of the haemorrhage," which the model supports.

Since the mathematical model for a phlebotomy simulates the data of Wadsworth [73] and Maeda *et al.* [47] fairly well, we might expect that the model could test alternative blood collection schemes and help enhance blood supplies of autologous donors. However, the data shown was a com-

posite of only 15 individuals. In Mahaffy *et al.* [49], two of the authors
enlisted the help of the San Diego Blood Bank to study their own response
to a blood donation with data collected very often for 8 weeks. These data
are shown in Fig. 4.3 overlaying the simulation of the mathematical model.
These data clearly do not have the same behavior as the averaged data of
Fig. 4.2 or the mathematical model. Only the initial trend of an immedi-
ate drop in the concentration of hemoglobin is consistent with the model,
and this is very short-lived with normal concentrations being observed 4–5
days after the phlebotomy. Soon the data follows an almost random pat-
tern with a mean of 14.66 and 15.10 (g/100 ml) for Mahaffy and Polk,
respectively. (The standard deviation was 0.86 and 0.91 for Mahaffy and
Polk, respectively.) The subjects of this study were not in a controlled
experiment, so their diet and exercise regimes varied significantly (though
measurements were taken at the same time each day). Careful analysis of
the data indicated that following heavy exercise (or SCUBA diving in one
case), the body adapts by lowering the concentration of hemoglobin. This
suggests a significant rapid response mechanism available to the body for
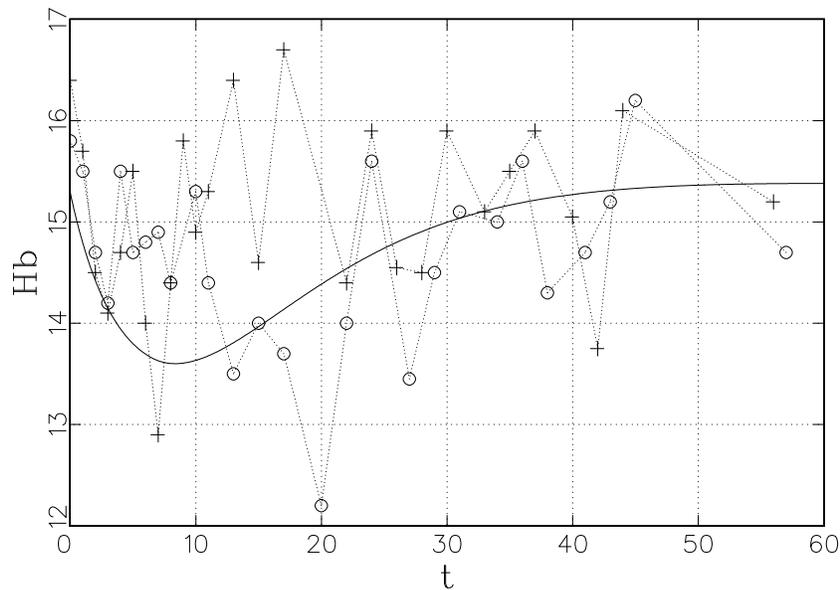increasing O_2 availability by diluting the blood, thus lowering its viscosity.

FIG. 4.3. *The solid curve shows the level of hemoglobin following a blood donation
predicted by the model. The data with ∘ are from the author Mahaffy, while the data
with + are from his collaborator Polk after a blood donation at $t = 0$.*

4.3. Variable Velocity of Aging. The weakest assumption is where the precursor cells age at a constant rate, which was used to reduce the age-structured model to a system of delay differential equations. Williams ([20], p. 436) claims that under extreme stress, the maturing stage of erythropoiesis is shortened. Studies using radioiron [21, 34, 38, 57] show that anemic conditions can decrease transit time (time of maturation) in the bone marrow for precursor cells by over a day and, furthermore, the stress of blood loss results in early release of "shift reticulocytes." Mahaffy *et al.* [49] use numerical methods based on the method of characteristics from Sulsky [68, 69] to simulate the age-structured model. The numerical simulations indicated that a variable velocity of aging could have profound stabilizing effect, especially in a diseased state. Bélair and Mahaffy [4] have proved this analytically by a linear analysis of reduced threshold-type delay equations, resulting from the application of the method of characteristics to the age-structured model that includes $V(E)$. Biologically, this result implies that plasticity in the aging of hematopoietic precursor cells aids in stabilizing the populations of mature erythrocytes, which should help maintain constant supplies of O_2 to the tissues.

5. Discussion. This review article demonstrates how age-structured models can be applied to a variety of problems in hematopoiesis. The mathematical models provide a valuable tool for examining hematopoietic diseases. Our study of the experiment by Orr *et al.* [56] for an induced auto-immune hemolytic anemia in rabbits demonstrated that the qualitative behavior can be simulated reasonably well by adjusting a parameter in the model corresponding to the increased random destruction of erythrocytes by the injected iso-antibody. Additional studies of the physiological parameters in the mathematical model could provide insight into the causes of other hematopoietic diseases or could suggest appropriate therapies for improving the condition of the animal.

Our study of the age-structured model for erythropoiesis following a phlebotomy in normal males gave mixed results. We were able to match averaged data for a collection of subjects, but the model was not a good means of predicting the hemoglobin concentrations in an individual. The study of Mahaffy *et al.* [49] indicates a need to better understand the exchange of plasma and the role of viscosity in blood to the varying needs of O_2 in the tissues. This modeling effort shows the complexity of the physiological controls that have evolved for this crucial O_2 delivery system. Our simplified mathematical model fails to adequately explain the adaptations required by the circulatory system to the external environment.

The studies of Mahaffy *et al.* [49] and Bélair and Mahaffy [4] on the variable velocity of aging for the precursor cells showed an increase in stability of the mathematical model. This suggests that animals have developed a plasticity in their hematopoietic systems in the early stages of development in order to maintain a homeostasis. The analysis of the complete

age-structured model demonstrates the importance of certain evolutionary
adaptations that the simpler delay differential equations models cannot
detect.

Mathematically, Bélair *et al.* [3] and Mahaffy *et al.* [48] determined
the assumptions necessary to connect the more complicated age-structured
models, *e.g.*, Grabosch and Heijmans [29] and Metz and Diekmann [52], to
the simpler delay differential equation models, *e.g.*, Bélair and Mackey [2].
The simpler delay differential equations allow a more complete analysis and
are computationally easier for testing parameters. Yet they are adequate
for understanding many aspects of the biological controls, especially in
certain diseased states.

REFERENCES

[1] J. Bélair. Stability analysis of an age-structured model with a state-dependent
delay. *Can. Appl. Math. Quart.*, 6:305–319, 1998.

[2] J. Bélair and M. C. Mackey. A model for the regulation of mammalian platelet
production. *Ann. N. Y. Acad. Sci.*, 504:280–282, 1987.

[3] J. Bélair, M. Mackey, and J. M. Mahaffy. Age-structured and two-delay models for
erythropoiesis. *Math. Biosci.*, 128:317–346, 1995.

[4] J. Bélair and J. M. Mahaffy. Parameter sensitivity in hematopoietic models.
Preprint 1999.

[5] J. Bernard and J. Caen. Purpura thrombopenique et megacaryocytopenie cycliques
mensuels. *Nouv. Rev. franc. Hemat.*, 2:378–386, 1962.

[6] O. Brey, E. P. R. Garner, and D. Wells. Cyclic thrombocytopenia associated with
multiple antibodies. *Brit. Med. J.*, 3:397–398, 1969.

[7] E. L. Burwell, B. A. Brickley, and C. A. Finch. Erythrocyte life span in small
mammals. *Amer. J. Physiol.*, 172:718, 1953.

[8] J. Caen, G. Meshaka, M. J. Larrieu, and J. Bernard. Les purpuras thrombopeniques
intermittents idiopathiques. *Sem. Hop. Paris*, 40:276–282, 1964.

[9] G. Chikkappa, G. Borner, H. Burlington, A. D. Chanana, E. P. Cronkite, S. Ohl,
M. Pavelec, and J. S. Robertson. Periodic oscillation of blood leukocytes,
platelets, and reticulocytes in a patient with chronic myelocytic leukemia.
Blood, 47:1023 –1030, 1976.

[10] T. Cohen and D. P. Cooney. Cyclical thrombocytopenia: Case report and review
of literature. *Scand. J. Haemat.*, 12:9–17, 1974.

[11] J. M. Cushing. Structural population dynamics. In S.A. Levin, editor, *Frontiers
in Theoretical Biology. Volume 100, Lecture Notes in Biomathematics*, pages
280–295. Springer-Verlag, Berlin and New York, 1994.

[12] D. C. Dale, D. W. Alling, and S. M. Wolff. Cyclic hematopoiesis: The mechanism
of cyclic neutropenia in grey collie dogs. *Journal of Clinical Investigation*,
51:2197–2204, 1972.

[13] D. C. Dale and W. P. Hammond. Cyclic neutropenia: A clinical review. *Blood
Reviews*, 2:178–185, 1988.

[14] J. Delobel, P. Charbord, P. Passa, and J. Bernard. Evolution cyclique spontanee
de la leucocytose dans un cas de leucemie myeloide chronique. *Nouv. Rev. Fr.
Hematol.*, 13:221–228, 1973.

[15] T. Demmer. Morbus maculosus werlhofii in regelmassigen vierwochentlichen

schuben bei einem 60 jahrigen mann, nebst untersuchungen uber die blut-plattchen. *Folia Haemat.*, 26:74–86, 1920.

[16] O. Diekmann and J. A. J. Metz. On the reciprocal relationship between life histories and population dynamics. In S.A. Levin, editor, *Frontiers in Theoretical Biology. Volume 100, Lecture Notes in Biomathematics*, pages 19–22. Springer-Verlag, Berlin and New York, 1994.

[17] C. D. R. Dunn. Cyclic hematopoiesis: The biomathematics. *Experimental Hematology*, 11:779–791, 1983.

[18] K. Engstrom, A. Lundquist, and N. Soderstrom. Periodic thrombocytopenia or tidal platelet dysgenesis in a man. *Scand. J. Haemat.*, 3:290–292, 1966.

[19] A. J. Erslev. Erythropoietin titers in health and disease. *Seminars in Hematology*, 28 Sup.3:2–8, 1991.

[20] A. J. Erslev and E. Beutler. Production and destruction of erythrocytes. In E. Beutler, M. A. Lichtman, B. S. Coller, and T. J. Kipps, editors, *William's Hematology*, chapter 39. McGraw-Hill Inc., New York, 5th edition, 1995.

[21] C. A. Finch, L. A. Harker, and J. D. Cook. Kinetics of the formed elements of human blood. *Blood*, 50:699–707, 1977.

[22] P. Fortin and M. C. Mackey. Periodic chronic myelogenous leukaemia: Spectral analysis of blood cell counts and aetiological implications. *Br. J. Haemato.*, 104:336–345, 1999.

[23] J. A. Gatica and P. Waltman. A threshold model of antigen antibody dynamics with fading memory. In V. Lakshmikantham, editor, *Nonlinear Phenomena in Mathematical Sciences*. Academic Press, New York, 1982.

[24] J. A. Gatica and P. Waltman. A system of functional differential equations modeling threshold phenomena. *Appl. Anal.*, 28:39–50, 1988.

[25] R. A. Gatti, W. A. Robinson, A. S. Deinare, M. Nesbit, J. J. McCullough, M. Ballow, and R. A. Good. Cyclic leukocytosis in chronic myelogenous leukemia. *Blood*, 41:771–782, 1973.

[26] L. Glass and M. C. Mackey. Pathological conditions resulting from instabilities in physiological control systems. *Ann. N. Y. Acad. Sci.*, 316:214–235, 1979.

[27] B. Goldschmidt and R. Fono. Cyclic fluctuations in platelet count, megakaryocyte maturation and thrombopoietin activity in cyanotic congenital heart disease. *Acta. Paediat. Scand.*, 61:310–314, 1972.

[28] R. R. Gordon and S. Varadi. Congenital hypoplastic anemia (pure red cell anemia) with periodic erythroblastopenia. *Lancet*, i:296–299, 1962.

[29] A. Grabosch and H. J. A. M. Heijmans. Cauchy problems with state-dependent time evolution. *Japan J. Appl. Math.*, 7:433–457, 1990.

[30] A. Grabosch and H. J. A. M. Heijmans. Production, development and maturation of red blood cells. A mathematical model. In D.E. Axelrod O. Arino and M. Kimmel, editors, *Mathematical Population Dynamics*, pages 189–210. Marcel Dekker, New York, 1991.

[31] W. S. C. Gurney and R. M. Nisbet. The systematic formulation of delay-differential models of age or size structured populations. In H. I. Friedman and C. Strobeck, editors, *Population Biology*, Volume 52, Lecture Notes in Biomathematics. Springer-Verlag, Berlin, 1983.

[32] C. Haurie, D. C. Dale, and M. C. Mackey. Cyclical neutropenia and other periodic hematological disorders: A review of mechanisms and mathematical models. *Blood*, 92:2629–2640, 1998.

[33] T. Hearn, C. Haurie, and M. C. Mackey. Cyclical neutropenia and the peripheral control of white blood cell production. *J. theor. Biol.*, 192:167–181, 1998.

[34] R. S. Hill. Characteristics of marrow production and reticulocyte maturation in normal man in response to anemia. *J. Clin. Invest.*, 48:443–453, 1969.

[35] J. B. Jones and R. D. Lange. Cyclic hematopoiesis: Animal models. *Immunology and Hematology Research Monographs*, 1:33–42, 1983.

[36] B. J. Kennedy. Cyclic leukocyte oscillations in chronic myelogenous leukemia. *Blood*, 35:751–760, 1970.

[37] A. P. Korn, R. M. Henkelman, F. P. Ottensmeyer, and J. E. Till. Investigations of a stochastic model of haemopoiesis. *Exp. Hemat.*, 1:362–375, 1973.

[38] S. Labardini, Th Papayannopoulou, J. D. Cook, J. W. Adamson, R. D. Woodson, J. W. Eschbach, and R. S. Hill. Marrow radioiron kinetics. *Haematologia*, 7:301–312, 1973.

[39] R. D. Lange. Cyclic hematopoiesis: Human cyclic neutropenia. *Experimental Hematology*, 11:435–451, 1983.

[40] M. L. Lewis. Cyclic thrombocytopenia: A thrombopoietin deficiency? *J. Clin. Path.*, 27:242–246, 1974.

[41] C. A. Macken and A. S. Perelson. *Stem cell proliferation and differentiation*, Volume 76, Lecture Notes in Biomathematics. Springer-Verlag, Berlin, 1980.

[42] M. C. Mackey. Periodic auto-immune hemolytic anemia: An induced dynamical disease. *Bull. Math. Biol.*, 41:829–834, 1979.

[43] M. C. Mackey. Some models in hemopoiesis: Predictions and problems. In M. Rotenberg, editor, *Biomathematics and Cell Kinetics*, pages 23–38. Elsvier/North Holland, 1981.

[44] M. C. Mackey. Mathematical models of hematopoietic cell replication and control. In M. A. Lewis & J. C. Dalton H. G. Othmer, F. R. Adler, editor, *The Art of Mathematical Modeling: Case Studies in Ecology, Physiology & Biofluids*, pages 149–178. Prentice Hall, 1997.

[45] M. C. Mackey and L. Glass. Oscillation and chaos in physiological control systems. *Science*, 197:287–289, 1977.

[46] M. C. Mackey and J. G. Milton. Feedback, delays and the origin of blood cell dynamics. *Comments Theor. Biol.*, 1:299–327, 1990.

[47] H. Maeda, Y. Hitomi, R. Hirata, H. Tohyama, J. Suwata, S. Kamata, Y. Fujino, and N. Murata. The effect of phlebotomy on serum erythropoietin levels in normal healthy subjects. *Int. J. Hemat.*, 55:111–115, 1992.

[48] J. M. Mahaffy, J. Bélair, and M. Mackey. Hematopoietic model with moving boundary condition and state dependent delay: Applications in erythropoiesis. *J. theor. Biol.*, 190:135–146, 1998.

[49] J. M. Mahaffy, S. W. Polk, and R. K. W. Roeder. An age-structured model for erythropoiesis following a phlebotomy. submitted to *Bul. Math. Biol.*, 1999.

[50] R. Mastrangelo, A. Stabile, D. Parenti, and G. Cimatti. A specific spontaneous leukocyte cycle in chronic myelogenous leukemia. *Tumori*, 62:197–204, 1976.

[51] R. Mastrangelo, A. Stabile, D. Parenti, and G. Segni. Spontaneous leukocyte oscillation during blastic crisis of chronic myeloid leukemia. *Cancer*, 33:1610–1614, 1974.

[52] J. A. J. Metz and O. Diekmann. *The Dynamics of Physiologically Structured Populations*, Volume 68, Lecture Notes in Biomathematics. Springer-Verlag, Berlin, 1986.

[53] A. Morley. Blood-cell cycles in polycythaemia. *Aust. Ann. Med.*, 18:124–126, 1969.

[54] T. Nakahata, A. J. Gross, and M. Ogawa. A stochastic model of self-renewal and commitment to differentiation of the primitive hemopoietic stem cells in culture. *J. Cell. Physiol.*, 113:455–458, 1982.

[55] R. M. Nisbet and W. S. C. Gurney. The formulation of age-structured models. In T. G. Hallam and S. A. Levin, editors, *Mathematical Ecology*, Volume 17, Lecture Notes in Biomathematics. Springer-Verlag, Berlin, 1986.

[56] J. S. Orr, J. Kirk, K. G. Gray, and J. R. Anderson. A study of the interdependence of red cell and bone marrow stem cell populations. *Brit. J. Haemat.*, 15:23–34, 1968.

[57] Th Papayannopoulou and C. A. Finch. Radio-iron measurements of red cell maturation. *Blood Cells*, 1:535–546, 1975.

[58] P. Ranlov and A. Videbaek. Cyclic haemolytic anaemia synchronous with Pel-Ebstein fever in a case of Hodgkin's disease. *Acta Medica Scandinavica*, 174:583–588, 1963.

[59] H. A. Reimann. *Periodic Diseases*. F.A. Davis Company, Philadelphia, 1963.

[60] A. R. Rodriguez and C. L. Lutcher. Marked cyclic leukocytosis leukopenia in chronic myelogenous leukemia. *American Journal of Medicine*, 60:1041–1047, 1976.

[61] S. Schmitz, H. Franke, J. Brusis, and H. E. Wichmann. Quantification of the cell kinetic effects of G-CSF using a model of human granulopoiesis. *Exp. Hematol.*, 21:755–760, 1993.

[62] S. Schmitz, H. Franke, H. E. Wichmann, and V. Diehl. The effect of continuous G-CSF application in human cyclic neutropenia: A model analysis. *Br. J. Haematol.*, 90:41–47, 1995.

[63] S. Schmitz, M. Loeffler, J. B. Jones, R. D. Lange, and H. E. Wichmann. Synchrony of bone marrow proliferation and maturation as the origin of cyclic haemopoiesis. *Cell Tissue Kinet.*, 23:425–442, 1990.

[64] G. K. von Schulthess and N. A. Mazer. Cyclic neutropenia (CN): A clue to the control of granulopoiesis. *Blood*, 59:27–37, 1982.

[65] R. K. Shadduck, A. Winkelstein, and N. G. Nunna. Cyclic leukemia cell production in CML. *Cancer*, 29:399–401, 1972.

[66] W. A. Skoog, J. S. Lawrence, and W. S. Adams. A metabolic study of a patient with idiopathic cyclical thrombocytopenic purpura. *Blood*, 12:844–856, 1957.

[67] H. L. Smith. Reduction of structured population models to threshold-type delay equations and functional differential equations: A case study. *Math. Biosci.*, 113:1–23, 1993.

[68] D. Sulsky. Numerical solution of structured population models: I Age structure. *J. Math. Biol.*, 31:817–839, 1993.

[69] D. Sulsky. Numerical solution of structured population models: II Mass structure. *J. Math. Biol.*, 32:491–514, 1994.

[70] J. L. Swinburne and M. C. Mackey. Cyclical thrombocytopenia: Characterization by spectral analysis. Submitted to *J. Theor. Med.*, 1998.

[71] J. E. Till, E. A. McCulloch, and L. Siminovitch. A stochastic model of stem cell proliferation, based on the growth of spleen colony-forming cells. *Proc. Natl. Acad. Sci. USA*, 51:29–34, 1964.

[72] H. Vogel, H. Niewisch, and G. Matioli. Stochastic development of stem cells. *J. theor. Biol.*, 22:249–270, 1969.

[73] G. R. Wadsworth. Recovery from acute haemorrhage in normal men and women. *J. Physiol.*, 129:583–593, 1955.

[74] C. Wasastjerna. Cyclic thrombocytopenia of acute type. *Scand. J. Haemat.*, 4:380–384, 1967.

[75] T. E. Wheldon. Mathematical models of oscillatory blood cell production. *Math. Biosci*, 24:289–305, 1975.

[76] T. E. Wheldon, J. Kirk, and H. M. Finlay. Cyclical granulopoiesis in chronic granulocytic leukemia: A simulation study. *Blood*, 43:379–387, 1974.

[77] H. E. Wichmann and M. Loeffler. *Mathematical Modeling of Cell Proliferation: Stem Cell Regulation in Hemopoiesis*. CRC Press, Boca Raton, 1988.

[78] T. Wilkinson and B. Firkin. Idiopathic cyclical acute thrombocytopenic purpura. *Med. J. Aust.*, 1:217–219, 1966.

[79] D. G. Wright, D. C. Dale, A. S. Fauci, and S.M. Wolff. Human cyclic neutropenia: clinical review and long term follow up of patients. *Medicine*, 60:1 –13, 1981.

[80] D. G. Wright, R. F. Kenney, D. H. Oette, V. F. LaRussa, L. A. Boxer, and H. L. Malech. Contrasting effects of recombinant human grnulocyte-macrophage colony-stimulating factor (CSF) and granulocyte CSF treatment on the cycling of blood elements in childhood-onset cyclic neutropenia. *Blood*, 84:1257–1267, 1994.